ELSEVIER

Journal of Power Sources 90 (2000) 176–181

JOURNAL OF POWER SOURCES

www.elsevier.com/locate/jpowsour

Preparation and properties of $LiCo_yMn_xNi_{1-x-y}O_2$ as a cathode for lithium ion batteries

Masaki Yoshio [a], Hideyuki Noguchi [a,*], Jun-ichi Itoh [a], Masaki Okada [a], Takashi Mouri [b]

[a] *Department of Applied Chemistry, Saga University, Saga 840-8502, Japan*
[b] *Nanyoh Research Center, Tohso Co., Ltd., 4560 Kaisei, Shinnanyoh 746-0006, Japan*

Received 17 August 1999; received in revised form 16 January 2000; accepted 19 February 2000

Abstract

The preparation of $LiCo_yMn_xNi_{1-x-y}O_2$ from $LiOH \cdot H_2O$, $Ni(OH)_2$ and γ-MnOOH in air was studied in detail. Single-phase $LiCo_yMn_xNi_{1-x-y}O_2$ ($0 \leqq y \leqq 0.3$ and $x = 0.2$) is obtained by heating at 830–900°C. The optimum heating temperatures are 850°C for $y = 0$–0.1 and 900°C for $y = 0.2$–0.3. Excess lithium ($1 \leqq z \leqq 1.11$ for $y = 0.2$) and the Co doping level ($0.05 \leqq y \leqq 0.2$) do not significantly affect the discharge capacity of $Li_zCo_yMn_{0.2}Ni_{0.8-y}O_2$. The doping of Co into $LiMn_{0.2}Ni_{0.8}O_2$ accelerates the oxidation of the transition metal ion, and suppresses partial cation mixing. Since the valence of the manganese ion in $LiMn_{0.2}Ni_{0.8}O_2$ is determined to be 4, the formation of a solid solution between $LiCo_yNi_{1-y}O_2$ and Li_2MnO_3 is confirmed.

Keywords: Cathode material for lithium ion batteries; $LiCo_yMn_xNi_{1-x-y}O_2$; The valence of Mn in $LiCo_yMn_xNi_{1-x-y}O$; Optimum preparation temperature; Electrochemical property

1. Introduction

Layered $LiNiO_2$, which has been used as a cathode material, has a relatively low cost and high capacity when used in lithium ion batteries [1–9]; however, there are two important problems for such a cathode. One problem is the difficulty in the preparation of electroactive $LiNiO_2$ because its discharge capacity significantly depends on the Li/Ni ratio in Li_xNiO_2, partial cation mixing and the oxidation state of nickel. The other problem is the poor cycle life of the $LiNiO_2$ electrode when it is charged to a high voltage (4.3 V vs. Li^+/Li) for withdrawing a higher capacity.

We solved these problems by the substitution of Ni with Mn. $Li_zMn_{0.1}Ni_{0.9}O_2$ prepared in O_2 shows a constant discharge capacity of ca. 160 mA h/g over the wide range of z from 0.98 to 1.10 [10,11]. Capacity fading of this compound is lower than that of $LiNiO_2$. Furthermore, electroactive $LiMn_xNi_{1-x}O_2$ can be prepared in air for $x \geqq 0.2$ though its capacity decreases by about 10%.

A convenient way to overcome the relatively lower capacity of $LiMn_xNi_{1-x}O_2$ prepared in air would be the Co doping of $LiMn_xNi_{1-x}O_2$ because the presence of cobalt stabilizes the structure in a strictly two-dimensional fashion. We have found that the Co doping of $LiMn_{0.2}Ni_{0.8}O_2$ increases the discharge capacity when such compounds are prepared in air. In this paper, we report the optimum conditions for the synthesis of the electroactive $Li_zCo_yMn_xNi_{1-x-y}O_2$, its electrochemical properties and the valence of Mn in it.

2. Experimental

A manganese compound, γ-MnOOH (Tohso), was used as the manganese source. It is a very fine, needle-like particle with a 0.1–0.2 μm diameter. The cobalt source was Co_3O_4. $LiOH \cdot H_2O$ (2.06 g), $Ni(OH)_2$ (3.48 g), γ-MnOOH (0.88 g) and Co_3O_4 (0.20 g) were mixed ($y = 0.05$, and $x = 0.2$) and ground using a mortar and pestle. The mixture was then pressed at 800 kg/cm^2. The obtained disks were heated in air at 700–900°C for 20 h.

* Corresponding author. Tel.: +81-952-28-8674; fax: +81-952-28-8591.
E-mail address: noguchih@cc.saga-u.ac.jp (H. Noguchi).

0378-7753/00/$ - see front matter
PII: S0378-7753(00)00407-9

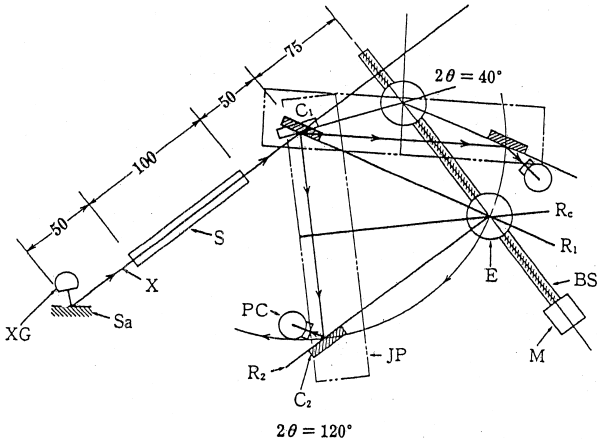

Fig. 1. Schematic diagram of two-crystal spectrometer. XG: X-ray generator; Sa: sample; X: X-ray; S: slit; C_1: first crystal; C_2: second crystal; R_1: first rail; R_2: second rail; R_c: center rail; JP: joint plate; PC: flow proportional counter; E: encoder; BS: ball screw; M: servomotor.

Crystallographic characterization of the samples was carried out using a Rigaku diffractometer (RINT 1000) with FeKα radiation. We used Izumi's Rietveld program (RIETAN) for the analysis of the powder diffraction profiles as previously reported [10,11].

High resolution fluorescence measurements of the $MnK_{\alpha 1}$ emission with a double crystal was done using a Technos XFRA190 X-ray fluorescence spectrometer as shown in Fig. 1. Disk samples made from manganese oxide powders were excited by a Rh target tube, and fluorescence spectra were measured using Ge (220) analyzer crystals and a slit of 1° for vertical divergence. The average oxidation numbers of the standard manganese oxide samples were determined by chemical analysis [12].

The charge/discharge characteristics of the $LiCo_yMn_xNi_{1-x-y}O_2$ cathodes were examined in laboratory cells. The cell was comprised of a cathode and lithium metal anode separated by a polypropylene separator and glass fiber mat. The cathode consisted of 20 mg of $LiCo_yMn_xNi_{1-x-y}O_2$ and 12 mg conducting binder pressed on a stainless steel screen at 800 kg/cm^2 and then dried at 200°C for 4 h. The electrolyte solution was 1 M $LiPF_6$/EC (ethylene carbonate) and DMC (dimethylcarbonate). The EC and DMC were mixed in a 1:2 volume ratio. The cell was cycled in the voltage range of 3.0–4.3 V at a current density of 0.4 mA/cm^2.

3. Results and discussion

3.1. Preparation of $LiCo_yMn_xNi_{1-x-y}O_2$ in air

We have already reported that the electroactive $LiMn_{0.2}Ni_{0.8}O_2$ with a discharge capacity of 140 mA h/g can be prepared in air containing CO_2 and moisture [10,11]. Cobalt is doped into the $LiMn_{0.2}Ni_{0.8}O_2$ system in order to increase the capacity because the doping of cobalt into the lithium–nickel oxide matrix stabilizes its layered structure [13].

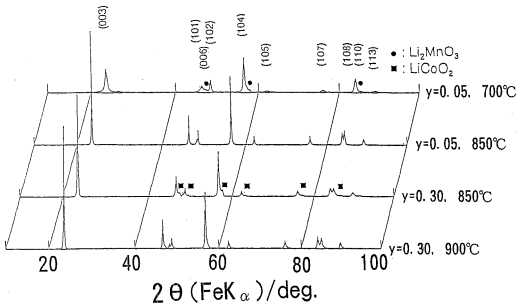

Fig. 2. XRD profiles of $LiCo_yMn_{0.2}Ni_{0.8-y}O_2$ samples ($y = 0.05$ and 0.30) prepared at various temperatures in air.

Fig. 2 shows the XRD patterns of the products obtained by heating the $LiOH \cdot H_2O$–$Ni(OH)_2$–γ-MnOOH–Co_3O_4 mixture at 700–900°C. The Li_2MnO_3 phase is recognized as an impurity at the lower heating temperature of 700°C for the lower Co doping level of $y = 0.05$ in $LiCo_yMn_{0.2}Ni_{0.8-y}O_2$; however, the peaks of the impurity phase completely diminish by heating at 850°C. When the heating temperature is not enough high, Li_2MnO_3 formed from LiOH and γ-MnOOH remains as an impurity because the formation of $LiMn_xNi_{1-x}O_2$ from Li_zNiO_2 and Li_2MnO_3 does not proceed smoothly at temperature lower than 850°C ($x = 0.2$) [10,11]. On the other hand, the peaks of the $LiCoO_2$ phase are observed for the sample ($y = 0.30$) heated at 850°C; however, this mixture becomes a single phase by heating at 900°C. As $LiMn_{0.2}Ni_{0.8}O_2$ is formed by heating at 850°C [10,11], $LiCo_yMn_{0.2}Ni_{0.8-y}O_2$ would be formed by the solid state reaction of $LiMn_{0.2}Ni_{0.8}O_2$ with $LiCoO_2$ at temperatures higher than 850°C. Single-phase $LiCo_yMn_{0.2}Ni_{0.8-y}O_2$ ($0 \leqq y \leqq 0.3$) with a space group $R_{\bar{3}m}$ can be successfully synthesized by heating the mixture at 830–900°C.

3.2. Structure characterization of $LiCo_yMn_{0.2}Ni_{0.8-y}O_2$ prepared in air

The hexagonal lattice parameters, *a* and *c*, of $LiCo_{0.05}Mn_{0.2}Ni_{0.75}O_2$ prepared in air at 700–900°C were determined by Rietveld refinement and are shown in Fig. 3. The samples heated at temperatures higher than 830°C

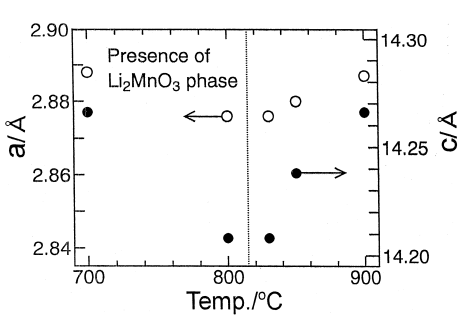

Fig. 3. The relation between the heating temperature and hexagonal lattice parameters, *a* and *c*, of $LiCo_{0.05}Mn_{0.2}Ni_{0.75}O_2$ samples.

are single-phase $LiCo_{0.05}Mn_{0.2}Ni_{0.75}O_2$; however, those heated at temperatures lower than 800°C contain a trace amount of Li_2MnO_3 as an impurity. Parameters *a* and *c* of the samples are the lowest at around 800–830°C, where they are 2.876 and 14.209 Å, respectively. The hexagonal unit cell volumes, calculated by $\sqrt{3}a^2c/2$, are also the lowest in this temperature range. Dahn et al. [1] reported that the cell volume of $Li_xNi_{2-x}O_2$ is the lowest for the ideal layered $LiNiO_2$. Based on their opinion, $LiCo_{0.05}Mn_{0.2}Ni_{0.75}O_2$ prepared at 800–830°C would be the closest to the ideal layered structure among them prepared at 700–900°C. The lowest c/a ratio at around 800–830°C would suggest the formation of a well-developed layered structure, since partial cation mixing in $LiCo_xNi_{1-x}O_2$ causes a decrease in the c/a ratio [14]. The heat treatment of $LiCo_{0.05}Mn_{0.2}Ni_{0.75}O_2$ at a higher temperature would cause cation mixing with the loss of oxygen as mentioned by Kanno et al. [7], so the *a*- and *c*-axes would expand by the heat treatment at higher temperature.

The lattice parameters, *a* and *c*, and c/a of $LiCo_y$-$Mn_{0.2}Ni_{0.8-y}O_2$ are illustrated as a function of *y* in Fig. 4. The heating temperatures of the samples are 850°C for $y = 0$, 0.05, and 0.10 and 900°C for $y = 0.20$ and 0.30, respectively. Both the *a*- and *c*-axes shrink with an increase in the Co doping level as was the case for $LiCo_yNi_{1-y}O_2$ [13,15,16]. The shrinkage of the *a*-axis in $LiCo_yMn_{0.2}Ni_{0.8-y}O_2$ at the lower Co doping levels ($0 \leqq y \leqq 0.1$) is smaller than that at the higher Co doping level ($0.1 < y \leqq 0.3$). On the other hand, the *c*-axis linearly shrinks with an increase in the Co doping level. Since the variation in the *c*-axis is only less than 0.2% and relatively smaller than that of the *a*-axis (1.6%), the variations in the c/a ratio and unit cell volume are mainly due to the shrinkage of the *a*-axis.

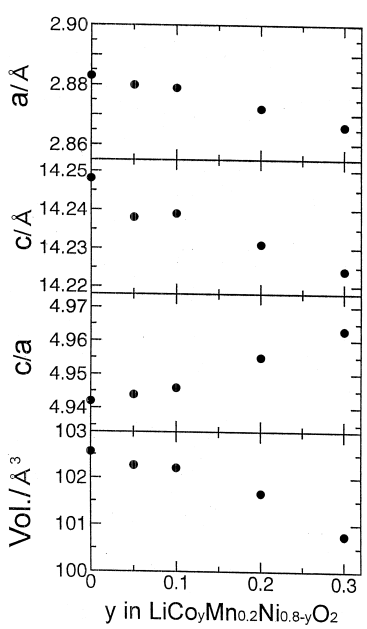

Fig. 4. Crystallographic data of single-phase $LiCo_yMn_{0.2}Ni_{0.8-y}O_2$ plotted as a function of *y*.

Table 1
Occupancies of metal ion (Co, Mn, Ni) in Li layer for various $LiCo_xMn_{0.2}Ni_{0.8-y}O_2$

Condition	*y*	Metal occupancies in Li layer (%)
850°C, 20 h, Air	0	7.2[a]
850°C, 20 h, Air	0.05	5.7
850°C, 20 h, Air	0.1	4.9
900°C, 20 h, Air	0.2	4.6
900°C, 20 h, Air	0.3	2.4

[a] Refs. [10,11].

The occupancies of the transition metal ion (Co, Ni, and Mn) in the lithium layer of $LiCo_yMn_{0.2}Ni_{0.8-y}O_2$ were determined by the Rietveld refinement and are summarized in Table 1. The occupancy of the transition metal ion in the lithium layer (3b site) decreases with an increase in the Co doping level. The occupancy in $LiCo_{0.3}Mn_{0.2}Ni_{0.5}O_2$ is only 1/3 and 1/2 of those in $LiMn_{0.2}Ni_{0.8}O_2$ prepared in air and O_2, respectively. This means that the Co doping of $LiMn_{0.2}Ni_{0.8}O_2$ is effective to stabilize the layered structure as was reported for $LiCo_xNi_{1-x}O_2$ [13].

3.3. Oxidation state of transition metal ion in $LiCo_y$-$Mn_{0.2}Ni_{0.8-y}O_2$

Fig. 5 shows the average valence of the transition metal ions in $LiCo_yMn_{0.2}Ni_{0.8-y}O_2$ prepared in air. It slightly increases from 2.92 to 2.98 with an increase in the Co doping level of $y = 0$–0.3; however, it is lower than that prepared in oxygen (3.05 at $y = 0$). If the valence of Co in them is assumed to be 3, the average valence of Ni and Mn will increase from 2.92 ($y = 0$) to 2.978 ($y = 0.3$). This means that Co would accelerate the oxidation of Ni and Mn. A nonlinear change at $y = 0.2$ would be caused by the elevated heating temperature of the samples with $y = 0.2$ and 0.3, since the decrease in the oxidation state of Ni in $LiNiO_2$ in air at temperatures higher than 700°C has been already confirmed by Yamada et al. [17].

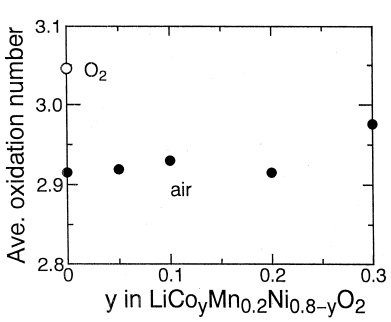

Fig. 5. Average oxidation number of $LiCo_yMn_{0.2}Ni_{0.8-y}O_2$ ($0 \leqq y \leqq 0.3$) prepared in air and $LiMn_{0.2}Ni_{0.8}O_2$ prepared under flowing O_2.

The chemical state analysis has become increasingly important, especially in the field of cathode materials for lithium-ion batteries. X-ray photoelectron spectroscopy, which is the most employed method, exploits the large efforts to estimate chemical state from the spectrum, and suffers from poor reliability of data, difficulty in application to bulk sample analysis and susceptibility to electrostatic effects such as energy shifts and curve distortion which require complex corrections. Therefore, for the bulk sample analysis, in particular, it is necessary to employ X-ray emission spectroscopy (XES). The effects of chemical state on the XES, however, are small, and hence, a high resolution X-ray fluorescence (HRXRF) spectrometer is required. We used an HRXRF spectrometer designed by Gohshi et al. [18].

The $MnK_{\alpha 1}$ (5898–5900 eV) spectra showed a chemical shift (deviation from metallic Mn in the energy of $K_{\alpha 1}$) and change in line profile. The measured parameters of the peak position, full-width at half-maximum (FWHM), and asymmetry index were calculated by the method described by Kawai et al. [19].

We found that the chemical shifts for various manganese oxides have a linear relation with the oxidation number of the Mn ion determined by the chemical analysis, as shown in Fig. 6. The chemical shifts of $LiMn_{0.1}Ni_{0.9}O_2$ and $LiMn_{0.2}Ni_{0.8}O_2$ (shown by ○) were found to be −0.15 to −0.17 eV, which are nearly equal to those (−0.14 to −0.21 eV) of the so-called manganese dioxide, such as β-, γ- and λ-MnO_2. The valences of Mn in $LiMn_xNi_{1-x}O_2$ are estimated to be 3.8–3.9, which is very close to 4. The FWHM of the $MnK_{\alpha 1}$ peak also depends on the oxidation state of Mn as mentioned [20]. The relationship between FWHM and the oxidation number of Mn for various manganese oxides is shown in Fig. 7. A linear relation is observed for the oxidation number of Mn from 3 to 4; however, the FWHM values of manganese dioxides and Li_2MnO_3 are scattered over the wide range

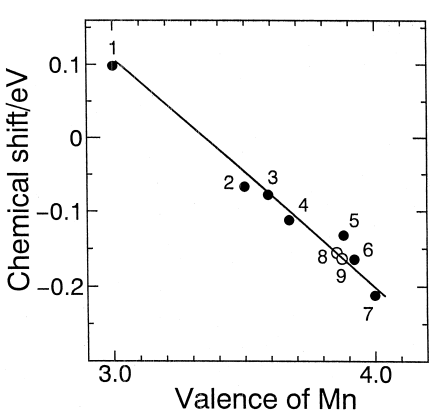

Fig. 6. The relation between the chemical shift of the $MnK_{\alpha 1}$ peak in HRXRF spectra and the valence of Mn for various manganese oxides. (1) γ-MnOOH, (2) $LiMn_2O_4$ prepared in N_2, (3) $LiMn_2O_4$ prepared in air, (4) $Li_{0.33}MnO_2$, (5) λ-MnO_2, (6) γ-Mn O_2, (7) β-MnO_2 and Li_2MnO_3, (8) $LiMn_{0.1}Ni_{0.9}O_2$, (9) $LiMn_{0.2}Ni_{0.8}O_2$.

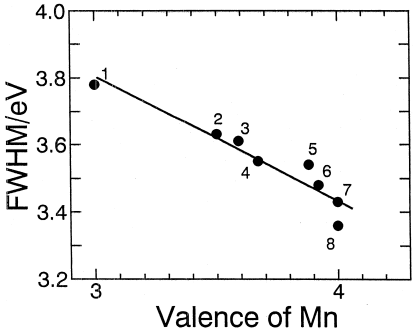

Fig. 7. The relation between FWHM of $MnK_{\alpha 1}$ peak and the valence of Mn for various manganese oxides. (1) γ-MnOOH, (2) $LiMn_2O_4$ prepared in N_2, (3) $LiMn_2O_4$ prepared in air, (4) $Li_{0.33}MnO_2$, (5) λ-MnO_2, (6) γ-MnO_2, (7) Li_2MnO_3, (8) β-MnO_2.

of 3.35–3.55 eV. The values of $LiCo_{0.05}Mn_{0.2}Ni_{0.75}O_2$ and $LiMn_{0.2}Ni_{0.8}O_2$ were determined to be 3.21–3.22 eV, which is lower than those (3.42–3.55 eV) of the manganese dioxides. However, they are close to that (3.35 eV) of Li_2MnO_3, which contains the tetravalent Mn ion. As described above, both the chemical shift and FWHM data would indicate that Mn in $LiCo_{0.05}Mn_{0.2}Ni_{0.75}O_2$ and $LiMn_{0.2}Ni_{0.8}O_2$ exist as a tetravalent ion.

Numata et al. [21] reported that layered $LiCoO_2$ forms a solid solution with Li_2MnO_3, and it is formulated as $Li(Co_{1-x}Li_{x/3}Mn_{2x/3})O_2$. Rossen et al. [22] also proposed that layered $LiNiO_2$ makes a solid solution with Li_2MnO_3. The valences of Mn in the solid solution should be 4, and then the HRXRF data for $LiCo_{0.05}Mn_{0.2}Ni_{0.75}O_2$ and $LiMn_{0.2}Ni_{0.8}O_2$ strongly support the formation of the solid solutions, $LiCo_yNi_{1-y}O_2$–Li_2MnO_3 and $LiNiO_2$–Li_2MnO_3. The formation of single-phase compounds, $Li_zMn_{0.1}Ni_{0.9}O_2$ ($0.98 \leqq z \leqq 1.10$) [10,11] and $Li_zCo_{0.05}Mn_{0.2}Ni_{0.75}O_2$ ($1 \leqq z \leqq 1.2$) also supports the fact that both $LiNiO_2$ and $LiCo_yNi_{1-y}O_2$ would form a solid solution with Li_2MnO_3.

The percentage of Ni(II) for total Ni in $LiMn_{0.2}Ni_{0.8}O_2$ can be calculated to be ca. 27%, when the valences of Co and Mn are assumed to be 3 and 4, respectively. The 3b site occupancies of the transition metal ions determined by the Rietveld analysis is less than 6%, so the occupancy of Ni(II) in the transition metal (Ni–Mn–Co) layer (3a site) is roughly 14%. This means that Ni(II) ion predominantly distributes in 3a site, which would be due to the presence of Mn in the 3a site because Ni(II) ion equally distributes 3a and 3b sites in $LiNiO_2$ [23] and $LiCo_xNi_{1-x}O_2$ [16].

3.4. Electrochemical behavior of $LiCo_yMn_{0.2}Ni_{0.8-y}O_2$

Fig. 8 shows the initial charge/discharge curves of $Li/LiCo_yMn_{0.2}Ni_{0.8-y}O_2$ ($y = 0.05$ and 0.30) electrodes at 0.4 mA/cm^2. The shapes of both curves are similar to each other; however, the delithiation of $LiCo_{0.3}Mn_{0.2}Ni_{0.5}O_2$ occurs at a slightly higher voltage than that

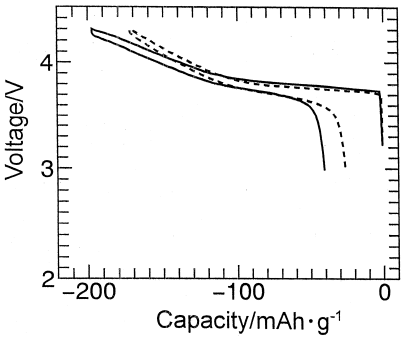

Fig. 8. Charge/discharge characteristics of $LiCo_{0.05}Mn_{0.2}Ni_{0.75}O_2$ (solid line) and $LiCo_{0.3}Mn_{0.2}Ni_{0.5}O_2$ (dashed line).

of $LiCo_{0.05}Mn_{0.2}Ni_{0.75}O_2$. The slope in the 3.9–4.3 V region increases with an increase in y of $LiCo_yMn_{0.2}Ni_{0.8-y}O_2$. The charge capacity (up to 4.3 V) decreased with an increase in the Co doping level because of its higher delithiation voltage. However, their irreversible capacity (difference between initial charge capacity and initial discharge capacity (down to 3.0 V)) also decreased with an increase in the Co doping level. These two effects of Co doping on the capacity cancel each other, and hence the discharge capacities of $LiCo_yMn_{0.2}Ni_{0.8-y}O_2$ ($0.05 \leqq y \leqq 0.3$) are kept roughly constant.

The initial discharge capacities of $LiCo_yMn_{0.2}Ni_{0.8-y}O_2$($0.05 \leqq y \leqq 0.3$) prepared at various heating temperatures are summarized in Table 2. The $LiCo_yMn_{0.2}Ni_{0.8-y}O_2$ ($0.05 \leqq y \leqq 0.1$) samples prepared at 830–850°C deliver a discharge capacity greater than 150 mA h/g. Their capacities are equal to that of $LiMn_{0.2}Ni_{0.8}O_2$ prepared under flowing O_2. This means that the doping of 5% Co allows us to prepare electroactive $LiMn_{0.2}Ni_{0.8}O_2$ in air.

The single-phase $LiCo_{0.3}Mn_{0.2}Ni_{0.5}O_2$ prepared at 900°C showed a slightly lower capacity than the sample with a lower Co doping level. This decrease in capacity is mainly due to a decrease in the charge capacity of $LiCo_{0.3}Mn_{0.2}Ni_{0.5}O_2$.

Though the discharge capacity of the $LiNiO_2$ cathode significantly decreases in the presence of an excess amount of Li, the $LiMn_xNi_{1-x}O_2$ cathode shows a constant discharge capacity at atomic ratios of the Li/transition metal from 0.98 to 1.10 [10,11]. This is an important property for the preparation of $LiMn_xNi_{1-x}O_2$ with a constant capacity in commercial production. Fig. 9 shows the relationship

Table 2
Discharge capacities of single-phase $LiCo_yMn_{0.2}Ni_{0.8-y}O_2$

Condition y	0	0.05	0.1	0.2	0.3
700°C, 20 h, Air	–	69	–	–	–
800°C, 20 h, Air	124	146	144	151	135
830°C, 20 h, Air	128	156	157	–	–
850°C, 20 h, Air	136	155	156	156	156
900°C, 20 h, Air	59	88	129	145	146

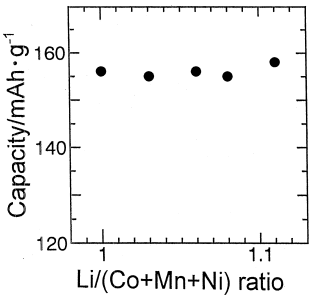

Fig. 9. Effect of Li content on the discharge capacity of $Li_zCo_{0.05}Mn_{0.2}Ni_{0.75}O_2$.

between the initial discharge capacity of $Li_zCo_{0.05}Mn_{0.2}Ni_{0.75}O_2$ and the Li/transition metal atomic ratio (z). Their discharge capacities do not depend on z and are roughly constant (155–158 mA h/g). This means that the addition of excess Li does not essentially affect the electrochemical property of $LiCo_{0.05}Mn_{0.2}Ni_{0.75}O_2$ as was reported for $LiMn_xNi_{1-x}O_2$ [10,11].

4. Conclusion

Electroactive $LiCo_yMn_{0.2}Ni_{0.8-y}O_2$ compounds with discharge capacities greater than 155 mA h/g were successfully prepared in air. The capacity was the same as that of $LiMn_{0.2}Ni_{0.8}O_2$ in oxygen. Excess lithium and the Co doping level $0.05 \leqq y \leqq 0.2$ did not significantly affect the discharge capacity of $Li_zCo_yMn_{0.2}Ni_{0.8-y}O_2$.

The doping of Co into $LiMn_{0.2}Ni_{0.8}O_2$ accelerated the oxidation of the transition metal ion and suppressed partial cation mixing. The valence of the manganese ion in $LiCo_{0.05}Mn_{0.2}Ni_{0.75}O_2$ was estimated to be 4, which indicates the formation of a solid solution between $LiCo_yNi_{1-y}O_2$ and Li_2MnO_3.

Acknowledgements

The authors would like to thank Mr. T. Konishi of the Asahi Chemical Analytical Research Laboratory for the measurement of the HRXRF spectra and Mr. S. Ikeda of the Saga University Instrumental Analysis Center for the use of their instruments. The present work was partly supported by a grant-in-aid for scientific research from the Ministry of Education, Science and Culture, Japan.

References

[1] J.R. Dahn, U. von Sacken, C.A. Michal, Solid State Ionics 44 (1990) 87.
[2] T. Ohzuku, A. Ueda, M. Nagayama, J. Electrochem. Soc. 140 (1993) 1862.
[3] W. Li, J.N. Reimers, J.R. Dahn, Solid State Ionics 67 (1993) 123.
[4] H. Arai, S. Okada, H. Ohtsuka, M. Ichimura, J. Yamaki, Solid State Ionics 80 (1995) 261.

[5] T. Miyashita, H. Noguchi, K. Yamato, M. Yoshio, J. Ceram. Soc. Jpn. 102 (1994) 58.
[6] J.R. Dahn, U. von Sacken, C.A. Michal, Solid State Ionics 44 (1990) 87.
[7] R. Kanno, H. Kubo, Y. Kawamoto, T. Kamiyama, F. Izumi, Y. Takeda, M. Takano, J. Solid State Chem. 110 (1994) 216.
[8] I. Davidson, J.E. Greedan, U. von Sacken, C.A. Michal, J.R. Dahn, Solid State Ionics 46 (1991) 243.
[9] H. Arai, S. Okada, H. Ohtsuka, Y. Sakurai, J. Yamaki, Solid State Ionics 95 (1997) 275.
[10] M. Yoshio, Y. Todorov, K. Yamato, H. Noguchi, J. Itoh, M. Okada, T. Mouri, J. Power Sources 74 (1998) 46.
[11] M. Yoshio, H. Noguchi, K. Yamato, J. Itoh, M. Okada, T. Mouri, Proc. Electrochem. Soc. 94-28 (1995) 251.
[12] M. Yoshio, J. Taira, H. Noguchi, K. Isono, Denki Kagaku 66 (1998) 335.
[13] E. Zhecheva, R. Stoyanova, Solid State Ionics 66 (1993) 143.
[14] Y. Choi, S. Pyun, S. Moon, Solid State Ionics 89 (1996) 43.
[15] C. Delmas, I. Saadoune, A. Rougier, J. Power Sources 43/44 (1993) 595.
[16] D. Caurant, N. Baffier, B. Garcia, J.P. Pereira-Ramos, Solid State Ionics 91 (1996) 45.
[17] S. Yamada, M. Fujiwara, M. Kanda, J. Power Sources 54 (1995) 209.
[18] Y. Gohshi, Y. Hukao, K. Hori, Spectrochim. Acta 27B (1972) 135.
[19] J. Kawai, E. Nakamura, Y. Nihei, K. Fujisawa, Y. Gohshi, Spectrochim. Acta 45B (1990) 463.
[20] Y. Gohshi, A. Ohtsuka, Spectrochim. Acta 28B (1973) 179.
[21] K. Numata, C. Sakaki, S. Yamanaka, Solid State Ionics 117 (1999) 257.
[22] E. Rossen, C.D.W. Jones, J.R. Dahn, Solid State Ionics 57 (1992) 311.
[23] R. Stoyanova, E. Zhecheva, C. Friebel, Solid State Ionics 73 (1994) 1.